J|A|C|S
ARTICLES
Published on Web 07/01/2003

Control of Redox Transitions and Oxygen Species Binding in Mn Centers by Biologically Significant Ligands; Model Studies with [Mn]-bacteriochlorophyll *a*

Idan Ashur,[†,§] Alex Brandis,[†] Moshe Greenwald,[†] Yahel Vakrat-Haglili,[†] Varda Rosenbach-Belkin,[†] Hugo Scheer,[‡] and Avigdor Scherz*[,†]

Contribution from the Department of Plant Sciences, The Weizmann Institute of Science, 76100 Rehovot, Israel and Botanisches Institut der Universität, D-80638 München, Germany

Received March 14, 2003; E-mail: avigdor.scherz@weizmann.ac.il

Abstract: Mn-superoxide dismutase (Mn-SOD), which protects the cell from the toxic potential of superoxide radicals ($O_2^{-\bullet}$), is the only type of SOD which resides in eukaryotic mitochondria. Up-to-date, the exact catalytic mechanism of the enzyme and the relationship between substrate moieties and the ligands within the active site microenvironment are still not resolved. Here, we set out to explore the possible involvement of hydroperoxyl radicals ($^\bullet$OOH) in the catalytic dismutaion by following the interplay of Mn^{III}/Mn^{II} redox transitions, ligands binding, and evolution or consumption of superoxide radical, using a new model system. The model system encompassed an Mn atom chelated by a bacteriochlorophyll allomer macrocycle (BChl) in aerated aprotic media that contain residual water. The redox states of the Mn ion were monitored by the Q_y electronic transitions at 774 and 825 nm for [Mn^{II}]- and [Mn^{III}]-BChl, respectively (Geskes, C.; Hartwich, G.; Scheer, H.; Mantele, W.; Heinze, J. *J. Am. Chem. Soc.* **1995**, *117*, 7776) and confirmed by electron spin resonance spectroscopy. Evolution of $^\bullet$OOH radicals was monitored by the ESR spin-trap technique using 5,5-dimethyl-1-pyrroline-*N*-oxide (DMPO). The experimental data suggest that the [Mn]-BChl forms a (HO^-)[Mn^{III}]-BChl(OOH) complex upon solvation. Spectrophotometeric titrations with tetrabutylamonnium acetate (TBAA) and 1-methylimidazole (1-MeIm) together with ESI-MS measurements indicated the formation of a 1:1 complex with [Mn]-BChl for both ligands. The coordination of ligands at low concentrations to [Mn^{III}]-BChl induced a release of a $^\bullet$OOH radical and a [Mn^{III}]-BChl → [Mn^{II}]-BChl transition at higher concentrations. The estimated equilibrium constants for the total redox reaction (K'_{tot}) are $1.9 \times 10^4 \pm 1 \times 10^3$ M^{-1} and 12.3 ± 0.6 M^{-1} for TBAA and 1-MeIm, respectively. The profound difference between the equilibrium constants agrees with the suggested key role of the ligand's basicity in the process. A direct interaction of superoxide radicals with [Mn^{III}]-BChl in a KO_2 acetonitrile (AN) solution also resulted in [Mn^{III}]-BChl → [Mn^{II}]-BChl transition. Cumulatively, our data show that the Mn^{III} center encourages the protonation of the $O_2^{-\bullet}$ radical in an aprotic environment containing residual water molecules, while promoting its oxidation in the presence of basic ligands. Similar coordination and stabilization of the $^\bullet$OOH radical by the Mn center may be key steps in the enzymatic dismutation of superoxide radicals by Mn-SOD.

Introduction

Manganese is specifically required for the regulation of reactive oxygen species (ROS) by enzymes such as superoxide dismutase (SOD) in prokaryotic mitochondria and in several types of bacterial catalase (Cat).[1,2] X-ray crystallography analyses of some SOD[1,3−6] and Cat[2,7] enzymes showed that the Mn atoms are ligated mainly by the imidazolic group of histidine and the carboxylic group of aspartate and glutamate, forming mono- or polynuclear metal centers. EXAFS and nuclear and electron paramagnetic resonance studies of wild type and mutated SOD and Cat at different redox states suggested that frequent association and dissociation of the Mn ions with the surrounding amino acid residues and solvent water molecules are apt to facilitate the redox changes of the Mn ion and/or binding of the ROS.[1,2,7−11]

The catalytic action of SOD enzymes aim to disarm the toxic potential of $O_2^{-\bullet}$ through the net dismutation reaction, $2O_2^{-\bullet} + 2H^+ \rightarrow H_2O_2 + O_2$. It is generally accepted that the catalytic dismutation is comprised of two elementary steps in which the metal acts as an electron acceptor and donor upon the incomming $O_2^{-\bullet}$ substrate:

[†] The Weizmann Institute of Science.
[‡] Botanisches Institut der Universität.
[§] In partial fulfillment of Ph.D. Thesis.

(1) Christianson, D. W. *Prog. Biophys. Mol. Biol.* **1997**, *67*, 217−252.
(2) Dismukes, G. C. *Chem. Rev.* **1996**, *96*, 2909−2926.
(3) Atzenhofer, W.; Regelsberger, G.; Jacob, U.; Peschek, G.; Furtmuller, P.; Huber, R.; Obinger, C. *J. Mol. Biol.* **2002**, *321*, 479−489.
(4) Borgstahl, G. E.; Parge, H. E.; Hickey, M. J.; Beyer, W. F., Jr.; Hallewell, R. A.; Tainer, J. A. *Cell* **1992**, *71*, 107−118.
(5) Edwards, R. A.; Baker, H. M.; Whittaker, M. M.; Whittaker, J. W.; Jameson, G. B.; Baker, E. N. *J. Biol. Inorg. Chem.* **1998**, *3*, 161−171.
(6) Fluckiger, S.; Mittl, P. R.; Scapozza, L.; Fijten, H.; Folkers, G.; Grutter, M. G.; Blaser, K.; Crameri, R. *J. Immunol.* **2002**, *168*, 1267−1272.
(7) Brunold, T. C.; Gamelin, D. R.; Stemmler, T. L.; Mandal, S. K.; Armstrong, W. H.; Penner-Hahn, H. E.; Solomon, E. I. *J. Am. Chem. Soc.* **1998**, *120*, 8724−8738.

10.1021/ja030170m CCC: $25.00

$$Mn^{III} + O_2^{-\bullet} \rightarrow Mn^{II} + O_2 \quad (1)$$

$$Mn^{II} + O_2^{-\bullet} + 2H^+ \rightarrow Mn^{III} + H_2O_2 \quad (2)$$

Interestingly, while Cu,Zn-SOD's are found in both the cytosol and the intermembranal space of the mitochondria, Mn-SOD is unique by being the only type of SOD which resides in the mitochondria matrix, and its defficiency or inactivity leads to cell death.[12−14] Although being a globular enzyme, recent studies pointed at the presence of Mn-SOD forms that are elctrostatically or covalently bound to the matrix inner-membrane boundary.[3,15,16] This localization may reflect a cellular strategy to treat superoxide radicals that are at different states of protonation, namely, $O_2^{-\bullet}$ or its protonated form hydroperoxyl ($^{\bullet}$OOH). The neutral or even slightly basic pH conditions in this domain seem to ensure the unprotonated nature of the $O_2^{-\bullet}$ substrate. However, this commonly accepted scheme may need some reconciliation. The multistep one electron transfer during respiration is coupled to proton translocation at a high rate. Additional proton translocation occurs in the coupled ATP synthesis.[17] As a result, superoxide radicals that form within the inner membrane are likely to be immediately protonated. The amphyphilic nature of the hydroperoxyl radicals allows their rapid mobilization in the lipid phase and subsequent partitioning between the membrane and matrix at the matrix/membrane boundaries as recently summarized by Muller et al. and de Grey et al.[16,17] The hydroperoxyl concentration at the matrix membrane boundary may not be sufficient for an efficient bimolecular nonenzymatic dismuation (as in the cytosolic membrane boundary, where localized low pH regions increases the $^{\bullet}$OOH concentratrion significantly),[16] but sufficiently high to interact with both the proteins and lipids. Thus, we raise the assumption that the matrix/inner-membrane bound Mn-SOD should facilitate an enzymatic dismutaion of both the protonated and unprotonated superoxide radical.

Several studies have pointed at the importance of protonation processes in controlling the redox potential of the enzyme.[18−21] Very recently, Han et al.[22] have studied the structural, energetic, and proton-coupled redox potentials of several wild-type and mutated Mn- and Fe-SOD enzymes. Their results show that Mn^{III}(Fe) is bound to OH^- and Mn^{II}(Fe) is bound to a water molecule. From the structural and energetic characteristics of Mn^{III}(Fe)OH^- and Mn^{II}(Fe)(H_2O) clusters, and the experimental rate constants, it was concluded that proton transfer happens in both steps of the catalytic cycle,

$$Mn^{III}(Fe^{III})(OH^-) + O_2^{-\bullet} + H^+ \rightarrow Mn^{II}(Fe^{II})(H_2O) + O_2 \quad (3)$$

$$Mn^{II}(Fe^{II})(H_2O) + O_2^{-\bullet} + H^+ \rightarrow Mn^{III}(Fe^{III})(OH^-) + H_2O_2 \quad (4)$$

This scheme differs from the conventional notion of the concomitant two protons transfer in the back oxidation step as depicted in eq 2. Particularly, it may suggest the participation of hydroperoxyl radicals in the catalytic cycle. Such participation may be an important step in superoxide dismutation, particularly at the mitochondria membrane boundary. Here, we set out to examine the putative formation and anihilation of hydroperoxyl during Mn^{II}/Mn^{III} transitions using Mn-bacteriochlorophyll allomer ([Mn]-BChl) as a model system. In this system, the Mn atom is chelated by a macrocycle that provides a more sensitive probe than the widely used porphyrin and phthalocyanine rings[23−25] for monitoring changes in the axial coordination and redox state of the chelated metal. Particularly, the nondegenerate electronic transitions provide the means to discriminate between different states of axial ligation and estimate concomitant changes in the metal ionic radius and redox state.[26−28] Hence, it is possible to investigate the chelated Mn^{II}/Mn^{III} interactions with oxygen radicals in the presence of ligands such as imidazole and acetate ion that represent the functional groups of histidine and aspartate or glutamate in Mn-SOD. These properties facilitate the investigation of the Mn-SOD key components interplay: redox transitions, coordinating ligands, and dioxygen moieties in aprotic environment that contain residual water. Our findings provide direct evidence for the evolution and utilization of hydroperoxyl radicals under conditions that may be relevant to Mn centers in SOD.

Materials and Methods

All solvents and reagents used were of analytical grade. Thin-layer chromatography (TLC) was performed on silica plates (Kieselgel 60 F264, Merck, Germany), using a chloroform−methanol (90:10, v/v) mixture for development. Column chromatography was done using silica (Kieselgel 60 H 0.063−0.200 μm and 0.040−0.063 m meshes, Merck, Germany), DEAE-Sepharose CL-6B, and CM-Sepharose CL-6B (Pharmacia Biotech, Sweden). 5,5-Dimethyl-1-pyrroline-*N*-oxide (DMPO) was purchased from Sigma and was washed on charcoal twice before application. All pigment manipulations were carried out under dim light conditions to prevent undesirable photochemical reactions.

Synthesis of 13²-Hydroxy-[Mn]-BChl by Transmetalation. BChl *a* was produced from *Rhodovulum sulfidophilum* (Phytol-based Bchl, MW 910 g/mole) and *Rhodospirrilum rubrum* (Geranylgeraniol-based Bchl, MW 904 g/mole) lyophilized bacteria using standard methods.[29−33]

(8) Renault, J. P.; Verchere-Beaur, C.; Morgenstern-Badarau, I. *Inorg. Chem.* **2000**, *39*, 2666−2675.
(9) Stemmler, T. L.; Sossong, T. M. J.; Goldstein, J. I.; Ash, D. E.; Elgren, T. E.; Kurtz, D. M. J.; Penner-Hahn, J. E. *Biochemistry* **1997**, *36*, 9847−9858.
(10) Hiraoka, B. Y.; Yamakura, F.; Sugio, S.; Nakayama, K. *Biochem. J.* **2000**, *345*, 345−350.
(11) Shank, M.; Barynin, V.; Dismukes, G. C. *Biochemistry* **1994**, *33*, 15433−15436.
(12) Fridovich, I. *Annu. Rev. Biochem.* **1995**, *64*, 113.
(13) Riley, D. P. *Chem. Rev.* **1999**, *99*, 2573.
(14) Rice-Evans, C., Halliwell, B., Lunt, G. G., Eds. *Free Radicals and Oxidative Stress: Environment, Drugs and Food Additives*; Portland Press: London, 1995.
(15) Okado-Matsumoto, A.; Fridovich, I. *J. Biol. Chem.* **2001**, *276*, 38388−38393.
(16) De Grey, A. *DNA Cell Biol.* **2002**, *21*, 251−257.
(17) Muller, F. *J. Am. Aging Assoc.* **2000**, *23*, 227−253.
(18) Leveque, V. J. P.; Stroupe, M. E.; Lepock, J. R.; Cabelli, D. E.; Tainer, J. A.; Nick, H. S.; Silverman, D. N. *Biochemistry* **2000**, *39*, 7131−7137.
(19) Vance, C. K.; Miller, A. F. *Biochemistry* **1998**, *37*, 5518−5527.
(20) Vance, C. K.; Miller, A. F. *J. Am. Chem. Soc.* **1998**, *120*, 461−467.
(21) Schwartz, A. L.; Yikilmaz, E.; Vance, C. K.; Vathyam, S.; Koder, R. L.; Miller, A. F. *J. Inorg. Biochem.* **2000**, *80*, 247−256.
(22) Han, W. G.; Lovell, T.; Noodleman, L. *Inorg. Chem.* **2002**, *41*, 205−218.
(23) Calvin, M. *Rev. Pure Appl. Chem.* **1965**, *15*, 1−11.
(24) Hoffman, B. M.; Szymanski, T.; Brown, T. G.; Basolo, F. *J. Am. Chem. Soc.* **1978**, *100*, 7254−7258.
(25) Lever, A. B. P.; Wilshire, J. P.; Quan, S. K. *J. Am. Chem. Soc.* **1977**, *101*, 3668−3677.
(26) Noy, D.; Fiedor, L.; Hartwich, G.; Scheer, H.; Scherz, A. *J. Am. Chem. Soc.* **1998**, *120*, 3684−3693.
(27) Noy, D.; Yerushalmi, R.; Brumfeld, V.; Ashur, I.; Scheer, H.; Scherz, A. *J. Am. Chem. Soc.* **2000**, *122*, 3937−3944.
(28) Yerushalmi, R.; Noy, D.; Baldrigde, K. K.; Scherz, A. *J. Am. Chem. Soc.* **2002**, *124*, 8406−8415.
(29) Ashur, I. M.Sc. Thesis, The Weizmann Institute of Science, Rehovot, Israel, 1999.

[For the purpose of this study, it is not necessary to distinguish between the two source skeleton.] The higher stability of BChl allomers (addition of oxygen atom at C-13^2 position) under aerobic conditions and light makes them more suitable for the study on oxygenic and nitrogenous coordination chemistry. Notably, no significant difference was found between the redox potentials and optical absorption of the [Mn]-BChl (Mn^{II} and Mn^{III}) and their corresponding allomers.[34] Allomerization of BChl and the following demetalation (central Mg atom removal) were performed as previously described. Purification of 13^2-hydroxybacteriopheophytin *a* (13^2-hydroxy-Bpheo) was carried out on a silica column (Kieselgel 60 H 0.040−0.063 m, Merck, Germany) with chloroform−*n*-hexane (1:1, v/v) as eluent. [The 13^2-hydroxy - designations will also be omitted throughout the rest of the manuscript.] [Mn]-BChl was synthesized by transmetalation as previously described.[35,36] Cadmium was inserted into Bpheo using a 10-fold molar excess of cadmium acetate in DMF at 110 °C under an inert atmosphere. The isolated [Cd]-BChl was dissolved in AC, and $MnCl_2 \cdot 2H_2O$ (2−3 molar excess) was added under stirring at room temperature. The reaction progress was monitored by probing the absorption spectra of mixture until completion (ca. 20 min in total). The AC was evaporated, and the pigment residues were twice redissolved in chloroform, decanted, and then dried by evaporating the chloroform. The procedure was repeated twice more with acetonitrile (AN), where decanted solution was additionally filtered through cotton wool. Finally, [Mn]-BChl was purified on silica column (Kieselgel 60 H 0.063−0.200 μm, Merck, Germany) with a gradient mixture 0−100% AC in chloroform, with 10% increment/100 mL. The purity of the fractions was examined by absorption spectra and thin-layer chromatography (silica gel, chloroform−methanol 4:1). Mass spectra of [Mn]-BChl in AN solution was obtained using the positive mode electrospray ionization mass spectrometer (LCZ, Micromass, England) and is presented in Figure 1a and b. The optical absorption of the purified complex appeared to be similar to the one assigned as [Mn^{III}]-BChl by Geskes et al. (Q_y at 824 nm).[34] The Mn incorporation could not proceed in the absence of molecular oxygen (when attempted to perform in a glovebox under N_2 atmosphere) using all other reagents as detailed above even after 1 h. However, when the mixture was exposed to the air, the reaction arrived at completion within ∼20 min, as under ordinary conditions.

UV/vis/NIR Absorption Measurements. [Mn]-BChl could be dissolved easily in AC to a concentration of several millimolar, showing neither degradation nor oxidation effects for several hours. Optical absorption spectra were recorded by a Jasco FP-750 (Jasco, Japan) spectrophotometer using a standard 1-cm optical path length quartz cuvettes that were sealed with a Teflon coated rubber stopper.

A. Treatment of [Mn]-BChl with Organic Ligands and Dithionite. Samples of [Mn]-BChl in AC (2000 μL, 15−20 μM) were titrated in a stepwise manner by 1-methylimidazole (1-MeIm, Sigma) and tetrabutylamonium acetate (TBAA, Alldrich). Stock solutions of the ligands were (1) 1-MeIm, 0.000 125−2.5 M, and (2) TBAA, 0.25 μM−25 mM. Typical aliqouts of 1−50 μL of the ligand were injected through the Teflon septum with a microliter syringe. The samples were left to equilibrate for ∼30 minutes between each consecutive measurement. The equilibrium constants were calculated from the changes in the absorbances at two different wavelengths by using the Hill method.[37] Sodium dithionite ($Na_2S_2O_4$) was dissolved in AC containing 15-crown-5-ether in excess (∼1000-fold).

B. Treatment of [Mn]-BChl with Superoxide in AN. The effect of supeoxide upon [Mn]-BChl was studied by using potassium superoxide (KO_2) as the source of the radical. Concentrations of several millimolar $O_2^{-\bullet}$ in aprotic solvents can be achieved by using 18-crown-6 ether while the radical was shown fairly stable in dimethyl sulfoxide (DMSO) and AN.[38,39] Here, we used KO_2/18-crown-6 ether in acetonitrile as a titrant for a sample of [Mn]-BChl in AN (5 μM in 2 mL of AN). The concentration of the radical was ∼330 μM as was determined by its UV absorption band at 252 nm ($\epsilon_{252} = 6.5\ mM^{-1}\ cm^{-1}$ in AN). The sample was titrated by 300 μL of KO_2 which corresponds to 10-fold titrant over the pigment.

Circular Dichroism Measurements. Circular dichroism spectra were recorded on an Aviv 202 CD recorder (Aviv Instruments Inc.) using a 1-cm path length rectangular quartz cell. The OD of the pigment was ∼0.8, corresponding to a concentration of ∼15 μM.

ESR Measurements. A. ESR Spectra of the Incorporated Manganese Ion. The ESR at 128.1 K was measured using a Bruker ESR ER 200 D-SRC spectrometer, equipped with a Bruker ER 040 XK Microwave X-band Bridge. The spectrometer was operated at 9.78 GHz, 39 mW microwave power, receiver gain of 1.25×10^5, and a scan time of 640 ms. Samples of 30 μM [Mn]-BChl in AC were partially reduced by adding aliquots of aqueous 0.06 M $Na_2S_2O_4$ solution. The contribution of [Mn^{III}]-BChl and [Mn^{II}]-BChl at each dithionite concentration was estimated from the optical absorption of the treated sample at 775 nm (and after correcting for the absorption of [Mn^{III}]-BChl at this wavelength). The relative growth of the ESR signal was estimated by integrating the area of the signal amplitude and was compared to the relative growth of the 775 nm band.

B. Spin-Trap Study. Qualitative identification of produced radical species resulting from the interaction of [Mn]-BChl with the studied ligands in aerated solutions was investigated by adding DMPO (80 mM) to samples of (a) [Mn]-BChl with 1-MeIm (140 μM and 800 mM, respectively) and (b) [Mn]-BChl with TBAA (100 μM and 5 mM, respectively). ESR spectra of the spin traps were recorded at 20 mW microwave power, 4×10^5 receiver gain, and 200 ms scan time, operated at 9.78 GHz. The optical absorption of each sample was recorded before and after the ESR measurement. ESR simulations were performed using the WinSim program of the NIEHS public ESR software package, available on the Internet (http://epr.niehs.nih.gov/pest.html).[40] The dependence of the ESR radical amplitude as a function of TBAA or 1-MeIm concentrations was measured at the same ligand concentration range that was used for the spectroscopic titrations (see above). Each sample contained 110 μL of a fixed pigment concentration (∼10 μM and different ligand concentrations together with 4 μL DMPO). The resulting signal was recorded at 20 mW microwave power, 4×10^5 receiver gain, 640 ms scan time, operated at 9.78 GHz. For each of the two titrations, the area of the signal amplitude was integrated and normalized according to the highest amplitude. The normalized values were compared to the extent of [Mn^{III}]-BChl decay, as determined from the corresponding absorbance of the samples at 825 nm.

Results

Redox Forms of [Mn]-BChl in Acetone. Table 1 summarizes the spectral properties of [Mn]-BChl in the presence of different reagents in AC and in AN. Figure 2 shows the spectrum of [Mn]-BChl in AC before and after the addition of sodium dithionite to the solution.

The major electronic transitions of [Mn]-BChl in AC are found at 825 (Q_y) and 615 nm (Q_x), typical to [Mn^{III}]-BChl.[34]

(30) Scheer, H.; Struck, A. In *The Photosynthetic Reaction Center*; Norris, J. R., Deisenhofer, J., Eds.; Academic Press: New York, 1993; pp 157−192.
(31) Struck, A.; Cmiel, E.; Katheder, I.; Schafer, W.; Scheer, H. *Biochim. Biophys. Acta* **1992**, *1101*, 321−328.
(32) Omata, T.; Murata, N. *J. Chromatogr.* **1983**, *316*, 24−41.
(33) Rosenbach-Belkin, V. Ph.D. Thesis, The Weizmann Institute of Science, Rehovot, 1988.
(34) Geskes, C.; Hartwich, G.; Scheer, H.; Mantele, W.; Heinze, J. *J. Am. Chem. Soc.* **1995**, *117*, 7776−7783.
(35) Scherz, A.; Salomon, Y.; Scheer, H.; Hartwich, G.; Brandis, A. Synthetic Metal Substituted Bacteriochlorophyll Derivatives and Use Thereof. U.S. Patent 6,333,319, 1997.
(36) Hartwich, G.; Fiedor, L.; Simonin, I.; Cmiel, E.; Schafer, W.; Noy, D.; Scherz, A.; Scheer, H. *J. Am. Chem. Soc.* **1998**, *120*, 3675−3683.
(37) Hill, H. A. O.; Macfarlane, A. J.; Williams, R. J. P. *J. Chem. Soc. A* **1969**, 1704.
(38) Ozawa, T.; Hanaki, A.; Yamamoto, H. *FEBS Lett.* **1977**, *74*, 79.
(39) Sawyer, D. T.; Calderwood, T. S.; Yamaguchi, K.; Angelis, A. *Inorg. Chem.* **1983**, *22*, 2577−2583.
(40) Duling, D. R. *J. Magn. Reson., Ser. B* **1994**, *104*, 105−110.

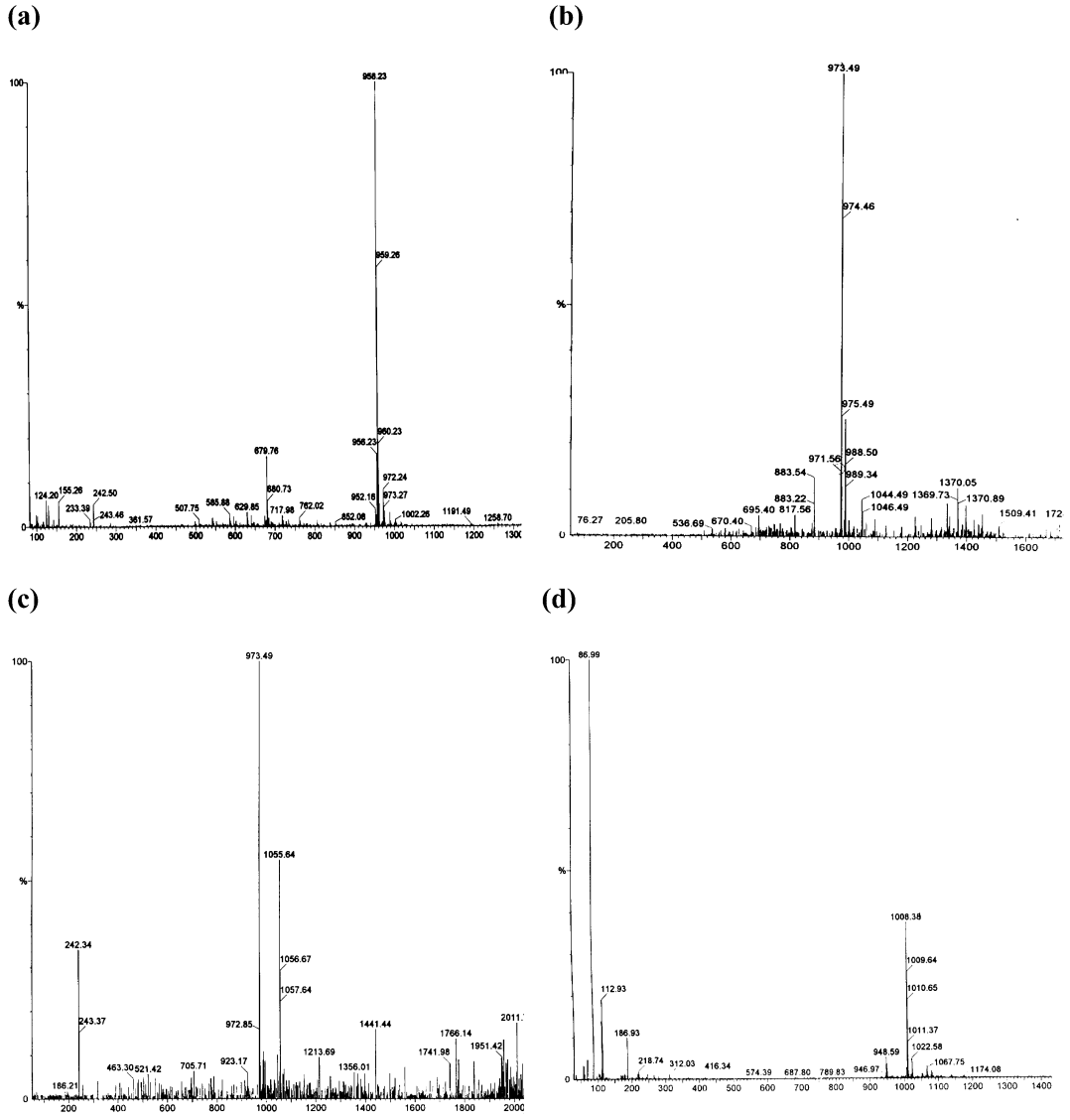

Figure 1. Electrospray ionization mass spectra of 13^2-hydroxy-[Mn]-BChl and its monocoordinated forms (a) phytol-based [Mn]-BChl, MW = 957 g/mol showing a peak at 958.2 *m*/*z* ([M + H]$^+$); (b) geranylgeraniol-based [Mn]-BChl, MW = 951 g/mol, showing a peak at 973.5 *m*/*z* ([M + Na]$^+$); (c) geranylgeraniol-based [Mn]-BChl coordinated to 1-MeIm, showing peaks at 973.5 *m*/*z* ([M + Na]$^+$) and at 1055.6 *m*/*z* ([M + 1-MeIm + Na]$^+$); and (d) geranylgeraniol-based [Mn]-BChl coordinated to an acetate anion showing a peak at 1008.4 *m*/*z* ([M-2 + acetate]$^-$. The operation mode was positive for samples a−c and negative for sample d. Sample d was cerfully examined by optical spectroscopy in order to confirm that the loss of 2 *m*/*z* units occurs within the ESI-MS apparatus and not as a result of degradation by chlorination of the product.

Table 1. UV/vis/NIR Spectral Properties of [Mn]-BChl

solvent	titrant	B_y (nm)	B_x (nm)	Q_x (nm)	Q_y (nm)
acetone	no titrant[a]	n.m.[b]	368 (41.2)[c]	615/8[d] (9.6)[c]	825/1[d] (52.7)[c]
	dithionite		372	601	775
	TBAA		372	608	780
	1-MeIm		372	597	780
acetonitrile	no titrant	326	366	601	821
	KO_2	∼332	371	574	766

[a] With no titrant, the spectrum contains additional LMCT at ∼472 and ∼520 nm. See the text for details. [b] Not measured due to large solvent absorption in that region. [c] Extinction coefficients in units of 10^3 M^{-1} cm^{-1} were found to be the same for both source skeleton products.[32] Pigment concentrations were determined by the ICP-AES technique as previously described.[29] [d] 615 and 825 for geranylgeraniol-based product; 618 and 821 for phytol-based product.

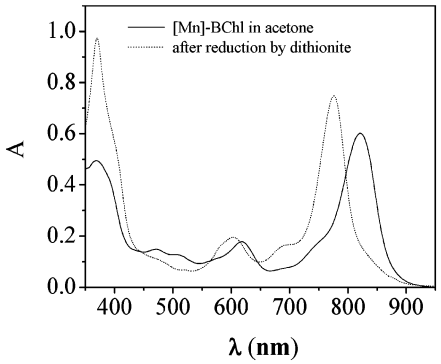

Figure 2. Spectral changes of [Mn]-BChl in acetone (bold line) upon the addition of dithionite (dotted line).

[615 and 825 for geranylgeraniol-based product; 618 and 821 for phytol-based product.] We propose that [Mn^{II}]-BChl in AC reacts with dioxygen and residual water to form a stable oxidized species *via* a two step reaction. First, axial coordination of

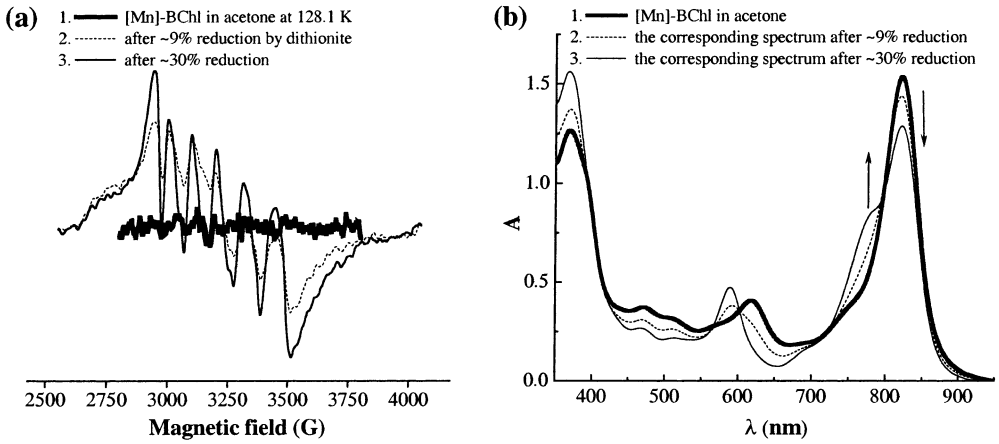

Figure 3. (a) X-band ESR spectrum of [Mn]-BChl in acetone at 128.1 K showing a stepwise reduction of the sample by dithionite and a corresponding increase of an Mn^{II} ion signal; (b) the corresponding optical spectra of the measured samples showing a clear correlation between the increase of the 775 nm band and the amount of divalent ion.

dioxygen and water molecules, which is concomitant to charge migration, form the metal to the dioxygen. This results in the formation of a coordinated superoxide moiety,[24,41]

$$[Mn^{II}]\text{-BChl} + O_2 + H_2O \rightleftharpoons (O_2^{-\bullet})[Mn^{III}]\text{-BChl}(H_2O) \quad (5)$$

Second, the ability of the superoxide anion to act as a strong Brønsted base in any medium ($HA + O_2^{-\bullet} \rightleftharpoons {}^{\bullet}OOH + A^-$)[42,43] couples the first step to form a stable cationic complex,

$$(O_2^{-\bullet})[Mn^{III}]\text{-BChl}(H_2O) \xleftrightarrow{H_2O} [(HOO)[Mn^{III}]\text{-BChl}]OH^- \quad (6)$$

Coordination of a hydroperoxyl moiety rather than a superoxide anion is thermodynamically favorable in view of the potentials of the involved redox couples. The potentials of $O_2/O_2^{-\bullet}$ and $O_2,H^+/{}^{\bullet}OOH$ redox couples in aprotic solvents are ca. -0.7 V and -0.017 V versus NHE,[44] respectively, while the redox potential of the $[Mn^{III}/Mn^{II}]$-BChl redox couple in AC was found to be -0.18 V (vs NHE).[45] Consequently $[Mn^{III}]$-BChl is expected to be reduced by $O_2^{-\bullet}$ but not by ${}^{\bullet}OOH$. Further thermodynamic stability of the bound hydroperoxyl moiety (i.e., a more positive redox potential) can be rationalized by accounting for its acid−base properties. Upon ligation to the central metal, the pK_a of ${}^{\bullet}OOH$ (4.86 in H_2O) is expected to increase as a result of the (d_{xz} or d_{yz})-π^* back-donation from the Mn^{III} center to the bound ${}^{\bullet}OOH$ moiety. On the other hand, as known for transition metal coordinated water molecules,[46,47] the pK_a of the coordinated water is expected to decrease because of charge migration from the lone pair oxygen electrons to the d_z^2 orbital of Mn^{III}. The overall effect is an enhanced stability of the Mn-hydroperoxyl complex in eq 6. Upon addition of dithionite, the Q_y and Q_x transitions shifted to 775 and 601 nm, respectively. The band at ~770−780 nm has been previously assigned to $[Mn^{II}]$-BChl.[34] A 601 nm transition was previously identified as the Q_x transition of the monoligated $[Mn^{II}]$-BChl allomer in diethyl ether.[36] The intensity of the two bands at ~472 and ~520 nm in $[Mn^{III}]$-BChl, assigned as ligand to metal charge transfer transitions (LMCT),[23,48−50] decreased upon the addition of dithionite, whereas the intensity of the B_x band at 372 nm is increased. A less resolved band appeared as a shoulder at ~410 nm. Accordingly, the end product of the reaction with dithionite is a reduced monoligated complex,

$$[(HOO)[Mn^{III}]\text{-BChl}]OH^- \xrightarrow{\text{dithionite}} (H_2O)[Mn^{II}]\text{-BChl} + \text{products} \quad (7)$$

Assessment of the $Mn^{III} \rightarrow Mn^{II}$ Transition by ESR Spectroscopy. Figure 3a shows the X-band (9.78 GHz) ESR signals of [Mn]-BChl in acetone at 128 K after treatment with different amounts of dithionite. Figure 3b shows the corresponding optical absorption spectra indicating ~9 and ~30% increases of the 775 nm spectral form.

Before treatment with dithionite, [Mn]-BChl (bold line) was "ESR-silent" as expected for a Mn^{III} high-spin (HS) d^4 ($S = 2$) configuration ("non-Kramers" ions) and similar to the one reported for $[Mn^{III}]$-Por compound.[50−53] The addition of dithionite resulted in the appearance of a six-line pattern ($H_r = \sim 3260$ G, $\Delta H_{pp} = \sim 100$ G) of the $^{55}Mn^{II}$ (HS d^5 configuration, $S = {}^5/_2$, $I = {}^5/_2$). This signal reflects the allowed $\Delta m_s = \pm 1$, $\Delta m_I = \pm 0$ transitions. Between the six main peaks, small features appear that arise from semiforbidden $\Delta m_I = \pm 1$ transitions that depend on second- and third-order effects. These effects involve zero field splitting terms.[54] Notably, no demetalated products of [Mn]-BChl were detected during the ESR measurements as indicated by the spectra in Figure 3b. The data in Table 2 indicate that the ratios of the integrated areas of the ESR signal and the respective ratios of the 775 nm band are in good

(41) Hoffman, B. M.; Weschler, C. J.; Basolo, F. *J. Am. Chem. Soc.* **1976**, *98*, 5473−5482.
(42) Chin, D. H.; Chiericato, G. J.; Nanni, E. J. J.; Sawyer, D. T. *J. Am. Chem. Soc.* **1982**, *104*, 1296.
(43) Roberts, J. L. J.; Sawyer, D. T. *Israel J. Chem.* **1983**, *23*, 430.
(44) Rodgers, M. A. J., Powers, E. L., Eds. In *Oxygen and Oxy-Radicals in Chemistry and Biology*; Academic Press: New York, 1981.
(45) Ashur, I.; Scherz, A. Unpublished data.
(46) Baes, C. F.; Mesmer, R. E. *The Hydrolysis of Cations*; Wiley: New York, 1976.
(47) Lippard, S. J.; Berg, J. M. *Principles of Bioinorganic Chemistry*; University Science Books: Mill Valley, California, 1994.
(48) Loach, P. A.; Calvin, M. *Biochemistry* **1963**, *2*, 361−371.
(49) Loach, P. A.; Calvin, M. *Biochim. Biophys. Acta* **1964**, *79*.
(50) Boucher, L. J. *Coord. Chem. Rev.* **1972**, *7*, 289−329.
(51) Yonetani, T.; Drott, H. R.; Leigh, J. J. S.; Reed, G. H.; Water, R. W. *J. Biol. Chem.* **1970**, *245*, 2998−3003.
(52) Goldberg, D. P.; Telser, J.; Krzystek, J.; Montalban, G. A.; Brunel, L. C.; Barrett, A. G. M.; Hoffman, M. B. *J. Am. Chem. Soc.* **1997**, *119*, 8722−8723.
(53) Boucher, L. J. *J. Am. Chem. Soc.* **1970**, *92*, 2725−2730.
(54) Reed, G. H.; Markham, G. D. *Biol. Magn. Reson* **1984**, *6*, 73−142.

Table 2. Correlation between the Increase of the 775 nm Band and the Corresponding ESR Signal of [Mn]-BChl upon Reduction by Dithionite

optical and ESR spectra number[a]	(2)	(3)
normalized absorption[b] peak at 774 nm	1	1.23
normalized area of the ESR amplitude[b]	1	1.18

[a] The numbering corresponds to the spectra numbers in Figure 3. [b] The data in the table are presented such that the absorption peak at 774 nm and ESR signal area are normalized relative to spectra 2 in Figure 3.

correlation. Namely, the growth of the [Mn^{II}]-BChl ESR signal is of the same extent as the growth of the 775 nm band. This provides evidence for the identification of the 775 nm form with the [Mn^{II}]-BChl redox state and supports eq 7.

Ligand Effects on [Mn]-BChl: Modification of the Redox States. Figure 4a and b shows the spectral changes induced upon the addition of acetate ion and 1-MeIm to [Mn^{III}]-BChl.

The similarity between the spectra at the end of the titrations and the spectrum of the dithionite treated sample infers that the addition of the ligands induced the reduction of the central metal. The Q_y band at 821 nm was replaced by a new band at 780 nm. The Q_x band blue shifted from 618 to 608 nm on adding TBAA and to 597 nm on adding 1-MeIm. The LMCT bands at ~474 and ~520 nm decreased. Isosbestic points were observed at 450, 574, 621, and 803 nm for TBAA. For 1-MeIm, clear isosbestic points could be observed at 614 and 654 nm in which the isosbestic properties were kept throughout the entire titration. Additional isosbestic points are featured at ~460 and ~530 nm in which the isosbesticity was deteriorated at high titrant concentrations, and the spectrospic transition at the Q_y region around ~800 nm lost its isosbestic properties already at early stages of the titration. We attribute the later features to the high concentrations of 1-MeIm that were used (up to 0.1 M and ~20 to ~50% v/v), which leads to the loss of "ideal-solution" conditions and which solvent effect upon the spectral properties of the pigment are much more severe. The B_x band at both samples, 372 nm increased. We propose that the observed reduction of [Mn^{III}]-BChl on adding ligands takes place through axial coordination which is followed by an acid−base and electron transfer reactions:

$$[(HOO)[Mn^{III}]\text{-BChl}]OH^- + L \rightleftharpoons [(L)[Mn^{III}]\text{-BChl}]OH^- + {}^{\bullet}OOH \qquad \beta_L \tag{8}$$

$${}^{\bullet}OOH + L \rightleftharpoons LH^+ + O_2^{-\bullet} \qquad K_a^{OOH}\cdot K_b^{L} \tag{9}$$

$$[(L)[Mn^{III}]\text{-BChl}]OH^- + O_2^{-\bullet} + LH^+ \rightleftharpoons (L)[Mn^{II}]\text{-BChl}(H_2O) + L + O_2\uparrow \qquad \frac{K_b^{L-M-OH}\cdot K^{ET}}{K_b^{L}} \tag{10}$$

In eqs 8−10, β_L is the stablity constant for the coordination of 1-MeIm; K_a^{OOH} and K_b^L are acidity and basicity equilibrium constants of ${}^{\bullet}OOH$ and L, respectively; K^{ET} stands for the homogeneous electron transfer equilibrium constant for the reduction of Mn^{III} to Mn^{II} by superoxide, and K_b^{L-M-OH} represents the basicity equilibrium constant of the ligated hydroxide anion. These equations should be somewhat modified for the case of the negatively charged acetate ion when considering its ability to act as a bidentate chelator,

$$[(HOO)[Mn^{III}]\text{-BChl}]OH^- + L^- \rightleftharpoons [(L^-)[Mn^{III}]\text{-BChl}] + {}^{\bullet}OOH \qquad \beta_L \tag{8a}$$

$${}^{\bullet}OOH + L^- \rightleftharpoons LH + O_2^{-\bullet} \qquad K_a^{OOH}\cdot K_b^{L} \tag{9a}$$

$$[(L^-)[Mn^{III}]\text{-BChl}] + O_2^{-\bullet} + LH \rightleftharpoons (LH)[Mn^{II}]\text{-BChl} + L^- + O_2\uparrow \qquad \frac{K_b^{L-M-OH}\cdot K^{ET}}{K_b^{L}} \tag{10a}$$

Such a scheme implies the possible occurrence of a "carboxylate shift" which describes a bidentate−monodentate transition of a metal-coordinated acetate ion and which was suggested to occur at several important biological Mn centers.[55,56]

When the exact forms of the species in each set of equations are disregarded, the equilibrium constant for the overall process is given by,

$$K_{tot} = \beta_L\cdot K_a^{OOH}\cdot K_b^{L-M-OH}\cdot K^{ET} = \frac{[(L)[Mn^{II}]\text{-BChl}(H_2O)]\cdot[O_2]}{[[(HOO)[Mn^{III}]\text{-BChl}]OH^-]\cdot[L]}$$

When working under atmospheric pressure, a pseudo equilibrium constant is obtained,

$$K'_{tot} = \frac{[(L)[Mn^{II}]\text{-BChl}(H_2O)]}{[[(HOO)[Mn^{III}]\text{-BChl}]OH^-]\cdot[L]}$$

Plots of $\log\{(A - A_0)/(A_f - A)\}$ vesrus log[L] were constructed for the 1-MeIm and TBAA titrations, where A is the absorbance at 830 nm, A_0 is the absorbance of [(HOO)-[Mn^{III}]-BChl]OH^- in the absence of ligand, and A_f is its absorbance at the end of the titration. Linear regression analyses of these plots are expected to yield a slope = 1, where $\log K'_{tot}$ can be estimated from the intercept. The plots are shown as insets in Figure 4, and the corresponding linear regression results are summarized in Table 3.

As expected from the equilibrium expression for $\log K'_{tot}$, the slopes for both titrations are in agreement with a 1:1 complex. Further support to this identification is given by the ESI-MS spectrum. A sample with 1-MeIm shows peaks at 973.5 *m*/*z* ($[M + Na]^+$) and at 1055.6 *m*/*z* ($[M + (1\text{-MeIm}) + Na]^+$) (Figure 1c), and the sample with TBAA shows a peak at 1008.4 *m*/*z* ($[M\text{-}2 + \text{acetate}]^-$) (Figure 1d). The values of $\log K'_{tot}$ for TBAA (4.3 ± 0.2) implies that $\log K'_{tot}$ for the reaction with TBAA is 4 orders of magnitudes larger than with 1-MeIm (1.09 ± 0.05). This probably originates from the fact that acetate is a better ligand for Mn^{III} (i.e., the contribution of β_L to $\log K'_{tot}$), but it might also reflect a dominant contribution of K_b^L to log K'_{tot} through K_b^{L-M-OH} (pK_b^L(acetate) = 9.25 and pK_b^L(1-MeIm) = 6.87). The coordinated acetate ion retains its ability to be protonated by converting its mode of ligation from bidentate to a monodentate ion, while the coordinated 1-MeIm has no available nitrogen that can serve as a proton donor. Thus, while the coordinated acetate can act as a strong base by itself, the influence of the 1-MeIm upon K_b^{L-M-OH} would be through charge density transfer to metal, an effect that is expected to be

(55) Carrell, C. J.; Carrell, J. E.; Erlebacher, J.; Glusker, J. P. *J. Am. Chem. Soc.* **1988**, *110*, 8651−8656.
(56) Steenhuis, J. J.; Hutchison, R. S.; Barry, B. A. *J. Biol. Chem.* **1999**, *274*, 14609−14616.

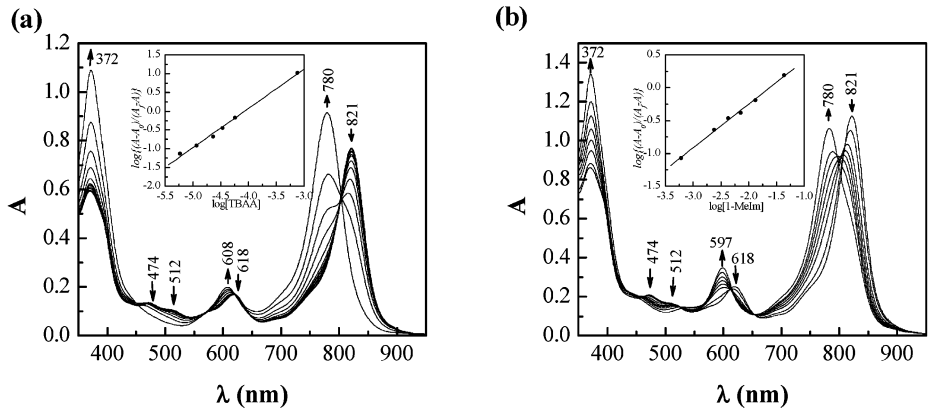

Figure 4. Spectroscopic titration of [Mn]-BChl in acetone with (a) TBAA; (b) 1-MeIm; the insets show the corresponding Hill plot for each titration from which the stoichiometries and $\log(K'_{tot})$ were extracted.

Table 3. Equilibrium Constants and Linear Regression Results for the Reaction of [Mn]-BChl with Acetate (OAc^-) and 1-MeIm as Were Extracted from the Corresponding Hill Plots of Figure 4

	slope	$\log(K'_{tot})$	R^2
(HOAc)[Mn^{II}]-BChl	1.05 ± 0.04	4.3 ± 0.2	0.9971
(1-MeIm)[[Mn^{II}]-BChl](H_2O)	0.68 ± 0.01	1.09 ± 0.05	0.9979

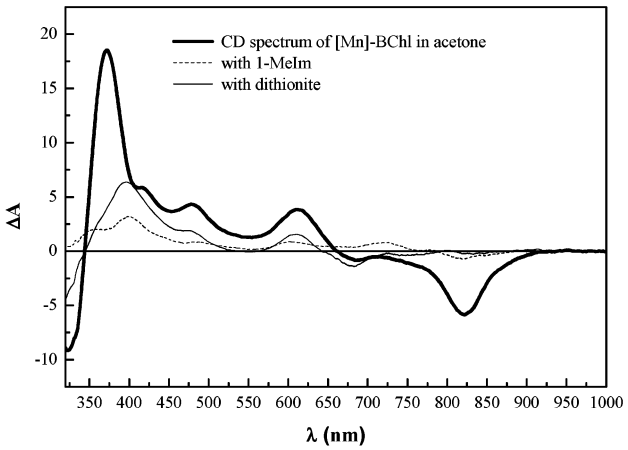

Figure 5. The effect of the addition of 1-MeIm and dithionite on the CD spectra of [Mn]-BChl in acetone; CD spectrum of [Mn]-BChl in acetone (bold line), after the addition of 1-MeIm (dotted line) and after the addition of dithionite (thin line).

relatively moderate. Investigation of this phenomenon by a series of ligands which enable to distinguish between the two effects and establish a quantitative relationship is under progress.

Ligand Effect on the Circular Dichroism Spectra of [Mn]-BChl. Geskes et al. and Hartwich et al. attributed the substantial red shift of the Q_y transition in [Mn^{III}]-BChl to the formation of μ-oxo-([Mn]-BChl)$_2$ dimers.[34,36] However, our CD results do not agree with this proposal. Figure 5 shows the CD of [Mn]-BChl before and after treatment with 1-MeIm or dithionite.

Before treatment, the Q_y band was negative and located at ~824 nm, whereas the Q_x transition at 611 nm and the charge transfer bands, located at 479 and 418 nm, showed a positive Cotton effect. The resolved B_x transition, located at 371 nm, was intense and positive in all samples. After treatment with dithionite or 1-MeIm, the ~824 nm optical transition was replaced by a 775 nm band and the overall CD intensity dramatically decreased. Notably, the dominant features in the CD spectra of an aggregated BChl are double Cotton effects of the corresponding electronic transitions.[33,57−60] Although samples of [Mn^{III}]-BChl exhibited a large bathochromic shift (~50 nm in AC), they did not show the oligomeric CD pattern. The overlap between the CD and optical absorption extrema and the absence of double Cotton effects around the individual transitions provide evidence for the monomeric nature of the spectral forms. The apparent decrease of the [Mn^{III}]-BChl CD signals upon metal reduction can be rationalized by considering conformational modifications of the macrocycle that probably result from the substantial changes in the metal's ionic radius upon ligation as previously reported for [Ni]-BChl in different states of ligation.[26,27]

Spin-Trap Detection of Hydroperoxyl Radical. To confirm the participation of the hydroperoxyl radical in the ligand induced reduction of [Mn^{III}]-BChl as suggested by eqs 8−10 and 8a−10a, we added the spin-trap agent DMPO to [Mn]-BChl in acetone before ligand titration. Under these conditions the addition of 1-MeIm or TBBA was accompanied by the appearance of broad EPR signals that are typical to the DMPO−OOH adduct (Figure 6).[61,62]

The latter intrepetation is strongly supported by simulation of the signal, presented as dotted lines in Figure 6. Figure 7 shows that the dependence of the DMPO−OOH signal intensity on the ligand concentration. A profound difference in the signal's trend can be observed on adding TBAA or 1-MeIm. On the other hand, the 821 nm intensity (reflecting the concentration of [(HOO)[Mn^{III}]-BChl]OH^-) decreased in a similar pattern for both ligands.

This observation is in agreement with eqs 8−10 and 8a−10 and with the difference between the estimated K'_{tot} values of the two ligands when considering a competition between DMPO and the ligand L over the released hydroperoxyl radical:

$$^{\bullet}OOH + L \rightleftharpoons LH^+ + O_2^{-\bullet} \qquad K_a^{OOH}\cdot K_b^L \qquad (9)$$

$$^{\bullet}OOH + DMPO \rightleftharpoons DMPO{-}OOH \qquad K_{DMPO} \qquad (11)$$

As long as $K_{DMPO}[DMPO] \gg \beta_L[L]$, the ligated Mn complex stays in the [(L)[Mn^{III}]-BChl]OH^- redox state. At increasing

(57) Scherz, A.; Rosenbach-Belkin, V. *Proc. Natl. Acad. Sci. U.S.A.* **1989**, *86*, 1505.
(58) Scherz, A.; Rosenbach-Belkin, V.; Fisher, J. R. E. *Proc. Natl. Acad. Sci. U.S.A.* **1990**, *87*, 5430.
(59) Brereton, G. R.; Sanders, K. M. *J. Chem. Soc., Perkin Trans. 1* **1983**, 423−430.
(60) Sauer, K.; Lindsay, J. R.; Schultz, A. J. *J. Am. Chem. Soc.* **1966**, *88*, 2681−2688.
(61) Evans, C. A. *Aldrichimica Acta* **1979**, *12*, 23.

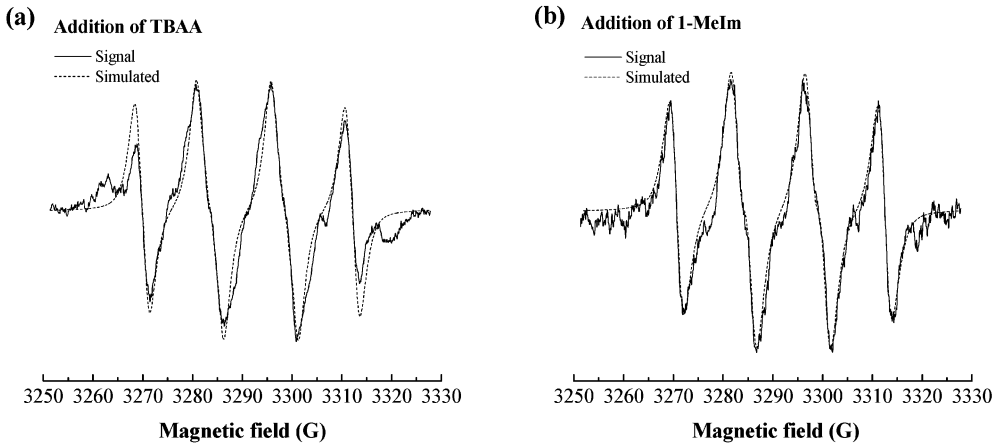

Figure 6. Experimental (solid line) and simulated (dotted line) ESR spectra of DMPO−OOH radical produced after the addition of ligands L to [Mn]-BCh in acetone: (a) L = OAc^-; calculated parameters $a_N = 14.90$ G, $a_H^\beta = 12.22$ G, $a_H^\gamma = 1.36$ and (b) L = 1-MeIm, calculated parameters $a_N = 14.98$ G, $a_H^\beta = 12.21$ G, $a_H^\gamma = 1.25$. Theoretical values for DMPO−OOH species: $a_N = 14.2$ G, $a_H^\beta = 11.3$ G, $a_H^\gamma = 1.25$ G.

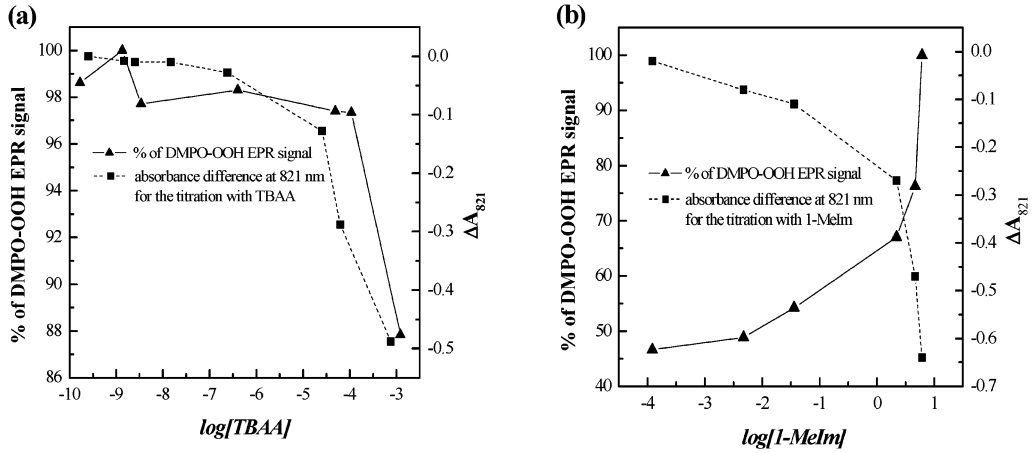

Figure 7. Comparison between the DMPO−OOH signal intensity (designated by the left vertical axes) and the 821 nm absorption intensity (designated by the right vertical axes): (a) titration with TBAA and (b) titration with 1-MeIm. Pigment and ligand concentrations were same as for the spectroscopic titrations shown in Figure 4.

concentrations of L, K_{DMPO}[DMPO] ≤ β_L[L] provided that β_L is large enough. In this concentration range, the •OOH radical undergoes deprotonation and reduces the [(L)[Mn^{III}]-BChl]OH^- complex according to eqs 9 and 10 or 9a and 10a. Thus, for ligands with low β_L values, we expect a steady increase of the DMPO−OOH signal intensity, whereas, for ligands with high β_L values, we expect a reduction of the DMPO−OOH signal at increasing ligand concentrations.

Interaction of [Mn]-BChl with Superoxide. The intereaction of [Mn]-BChl with $O_2^{-\bullet}$ were examined in an AN KO_2 solution. The spectral changes that are induced upon additon of the radical are depiced in Figure 8.

The spectra show similar changes to those observed on titrating [Mn^{III}]-BChl with dithionite. Particularly, the Q_y band shifted from 821 to 766 nm reflecting a $Mn^{III} \rightarrow Mn^{II}$ transition. It has been shown that the presence of acidic substrate (HA), which reacts as a Brønsted acid, accelerates the disproportionation of $O_2^{-\bullet}$ through a common mechanism, HA + $O_2^{-\bullet} \rightleftharpoons$ •OOH + A^-, •OOH + $O_2^{-\bullet} \rightarrow H_2O_2 + O_2$, and that this reaction depends on the acidity of HA.[42,63] Equations 5 and 6 suggest that the [Mn^{III}]-BChl complex acts as an inhibitor to this process by ligating the superoxide radical and

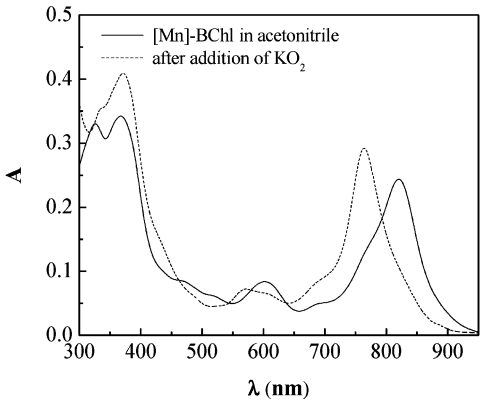

Figure 8. Spectral changes of [Mn]-BChl in AN (bold line) upon addition of potassium superoxide (dashed line).

forming the less acidic species, [(HOO)[Mn^{III}]-BChl]OH^- (i.e., pK_a(HOO−M−OH) > pK_a(•OOH)). However, if the solution initially contains mainly the [(HOO)[Mn^{III}]-BChl]OH^- species, then the $O_2^{-\bullet}$ might enhance the back reduction process through hydrolysis of water,

(62) Janzen, E. G.; Haire, D. L. *Adv. Free Radical Chem.* **1990**, *1*, 253.

(63) Che, Y.; Tsushima, M.; Matsumoto, F.; Takeyoshi, O.; Tokuda, K.; Ohsaka, T. *J. Phys. Chem.* **1996**, *100*, 20134−20127.

$$[(HOO)[Mn^{III}]\text{-BChl}]OH^- + O_2^{-\bullet} + H_2O \rightleftharpoons (O_2^{-\bullet})[Mn^{III}]\text{-BChl}(H_2O) + OH^- + {}^{\bullet}OOH \quad (12)$$

$$(O_2^{-\bullet})[Mn^{III}]\text{-BChl}(H_2O) \rightleftharpoons [Mn^{II}]\text{-BChl}(H_2O) + O_2\uparrow \quad (13)$$

This will enhance the overall effect of back reduction both by driving the equilibrium of eqs 5 and 6 to the left-hand side and by accelerating the disproportionation of $O_2^{-\bullet}$ ($^{\bullet}OOH + O_2^{-\bullet} \rightarrow H_2O_2 + O_2$ and/or $^{\bullet}OOH + {}^{\bullet}OOH \rightarrow O_2 + H_2O_2$).

Discussion

Superoxide radicals are continuously generated in the course of respiratory electron transfer. Since formation and propagation of these reactive oxygen species endanger vital components of the living cells, the mitochondrion is equipped with the Mn-SOD enzyme that detoxifies superoxide radicals by a high rate dismutation to hydrogen peroxide and dioxygen. Despite major research efforts, resolved architecture, and ample data concerning kinetics and thermodynamics of the Mn-SOD enzymes, the underlying principles of their catalytic activity are not fully resolved. First, the exact roles of the surrounding amino acid residues and the solvent molecules at the microenvironment of the active site have not been clarified to date. Second, the reflection of compartments within the mitochondria that differ by their pH and electric potential on the relative distribution of $O_2^{-\bullet}$ and $^{\bullet}OOH$ was not paid significant attention in the past. The majority of superoxide radicals generated during respiration within the mitochondria inner-membrane is in the form of $^{\bullet}OOH$ radicals which are dramatically more mobile then $O_2^{-\bullet}$ in a hydrophobic medium and, thus, can easily cross the membrane to both the matrix and the intermembrane space. Within the intermembrane space, localized low pH regions that are formed as the result of the ATP-synthase activity enhance the level of hydroperoxyl radicals to the extent that they can undergo an efficient bimolecular nonenzymatic dismutation.[16] This self-defense mechanism may not be applicable to the matrix side of the inner-membrane boundary. In this region, the anticipated concentration of the $^{\bullet}OOH$ radical might be sufficient to confer damage to surrounding proteins and membrane lipids but too low for an efficient bimolecular noncatalytic dismutation. Hence, scavenging of $^{\bullet}OOH$ radicals in the matrix/inner-membrane boundary relies only on enzymatic dismutation. Possibly, Mn-SOD might have the ability to interact with both $^{\bullet}OOH$ and $O_2^{-\bullet}$. In any event, the catalytic rate of substrate dismutation is assumed to depend on its coordination to the catalytic niche. Thus, major issues that await resolution regarding Mn-SOD activity relate with substrate identity and mode of coordination.

In this work we, addressed two topics: Mn-ligand interactions and Mn-ROS interactions using a novel model system. We have looked at the effect of biologically important ligands, namely, carboxylate and imidazole (the side residues most frequently coordinating Mn and Fe centers in SOD) on regulating redox reactions of Mn with oxygen species in aprotic solvents (AC or AN) containing residual water molecules. The low water concentration in these aprotic solvents together with ligands and superoxide radicals mimicked to a certain extent the Mn chemical environment within the protein niche of SOD. We present three key findings obtained under these conditions: (1) Mn^{III} binding to a hydroperoxyl radical provides a stable complex in aprotic solvents. (2) Axial coordination of nitrogenous or carboxylic groups releases the hydroperoxyl radical. (3) In the absence of a trapping site and in the presence of a Brønsted base, the hydroperoxyl radical undergoes deprotonation and becomes a reductive agent toward the Mn^{III} ion. Thus, an Mn^{III} center can promote the formation of a bound protonated $O_2^{-\bullet}$ radical in an aprotic environment containing a few water molecules, while catalyzing its oxidation in the presence of a basic ligand. The complete cycle for the proposed mechanism is presented in Scheme 1.

Scheme 1. Proposed Mechanism for the Promotion of Superoxide Radical Oxidation by [Mn]-BChl

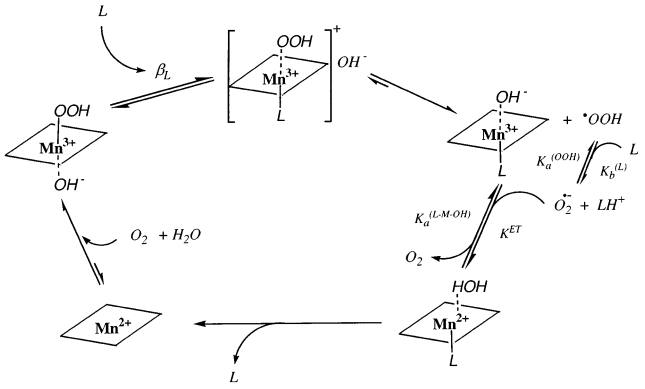

The interplay between oxidation and reduction of a superoxide radical is the essence of the Mn- and Fe-SOD catalytic activity. Recent studies underline the significance of superoxide protonation within the catalytic niche of Mn,Fe-SOD prior to reduction (by outer sphere electron transfer) on route to hydrogen peroxide formation. However, following the cumulative data presented by Miller et al.,[20,64,65] one may draw the conclusion that protonation may precede the binding of superoxide radical to the Mn^{III} center also in the first (inner electron transfer) catalytic step which involves substrate oxidation; for example,

$$(OH^-)Mn^{III} + O_2^{-\bullet} + H^+ \rightarrow (OH^-)Mn^{III}({}^{\bullet}OOH) \rightarrow (H_2O)Mn^{II} + O_2 \quad (14)$$

where the protein mediates the concomitant deprotonation of the substrate and protonation of the hydroxyl ion as observed in our model studies (eqs 5−10).

The advantage of this route is obvious. Coordination of Mn^{III} with a hydroperoxyl rather than a superoxide anion radical does not require any dramatic change of the metal configuration as it stays in the same redox state. This allows for practically an adiabatic transfer from the higher to the lower redox state during the inner electron transfer from the coordinated substrate to the metal. Further more, the proposed scheme allows for direct interactions of Mn-SOD with some hydroperoxyl radicals that migrate to the mitochondrion membrane/matrix interface. Future studies of SOD and model systems are expected to further clarify the link between the microenvironment of the Mn center and the formation of hydroperoxyl.

(64) Miller, A. F.; Schwartz, A. L.; Vance, C. K. *J. Inorg. Biochem.* **1999**, *74*, 41−41.
(65) Vance, C. K.; Miller, A. F. *Biochemistry* **2001**, *40*, 13079−13087.

Concluding Remark

We provide the first evidence that Mn^{III}/Mn^{II} transitions may lead to generation and quenching of hydroperoxyl radicals under conditions that resemble the immidiate environment of the Mn atom center in SOD. Our finding is in line with recent studies that call for researching this "forgotten radical"[16] as a potential key player of the ROS arsenal *in vivo* and re-evaluation of elementary catalytic steps of Mn- and Fe-SOD complexes.[22] We also proposed a link between our *in vitro* findings and recent considerations of the Mn-SOD mechanism of action. The possible contribution of the $^{\bullet}OOH$ radical to the catalytic rate of dismutation is a major subject of an ongoing study in our group.

Acknowledgment. This study was supported by the Deutsche Forschungsgemeinschaft, DFG-140 Grant, SFB Grant #533, US-ISR binational foundation (BSF) Grant #9800323/2, and the Avron-Minerva Center for Photosynthesis.

JA030170M